

Effect of ice cover on wave statistics and wave-driven processes in the northern Baltic Sea

Fatemeh Najafzadeh^{1)*}, Nadezhda Kudryavtseva¹⁾, Tarmo Soomere¹⁾²⁾ and Andrea Giudici¹⁾

¹⁾ Wave Engineering Laboratory, Department of Cybernetics, School of Science, Tallinn University of Technology, Akadeemia tee 21, Tallinn, 12618, Estonia
(*corresponding author's e-mail: fatemeh@ioc.ee)

²⁾ Estonian Academy of Sciences, Kohtu 6, Tallinn, 10130, Estonia

Received 11 Aug. 2021, final version received 21 Feb. 2022, accepted 17 Mar. 2022

Najafzadeh F., Kudryavtseva N., Soomere T. & Giudici A. 2022: Effect of ice cover on wave statistics and wave-driven processes in the northern Baltic Sea. *Boreal Env. Res.* 27: 97–116.

We explore the effect of sea ice on wind wave statistics and wave-driven hydrodynamic loads in a seasonally ice-covered sea. We compare the results of hypothetical ice-free wave simulations for 1979–2007 in the northern Baltic Sea with *in-situ* wave time series and with truncated simulations in which waves during the ice season are ignored. The ice cover impacts the mean wave properties usually less than 5% and up to 10–20% at a few locations. The cumulative annual wave energy and energy flux are greatly (up to 82%) influenced. The mean wave properties and the ice season duration are almost uncorrelated in the Sea of Bothnia and Bay of Bothnia but have a statistically significant (at a > 99% level) negative correlation at the latitudes of the Gulf of Finland. This feature implies that climate-driven changes, first of all, the later appearance of ice in the relatively windy late autumn and winter season, may considerably add energy to coastal processes at these latitudes.

Introduction

Variations in the wave climate have a broad impact, from shaping coastlines (e.g., Łabuz 2015, Kelpšaitė-Rimkienė *et al.* 2021) and coastal erosion (Ryabchuk *et al.* 2011, Suursaar *et al.* 2014, Harff *et al.* 2017) to the safety of navigation and shipping (Goerlandt *et al.* 2017, Lensu and Goerlandt 2019). These variations are largely driven by similar variations in the weather conditions, first of all wind forcing and air temperature. Sea ice also has a great influence on wave properties. They both have extensive seasonal and interannual variability and they both are eventually impacted by climate change

in boreal marginal seas, such as the Baltic Sea (Fig. 1).

The weather conditions of the Baltic Sea are mostly controlled by two dominant atmospheric circulation systems; the North Atlantic Oscillation and the Scandinavian mode (e.g., von Storch *et al.* 2015). Their extensive variability leads to large spatial and temporal variations in the mean and extreme Baltic Sea wave properties. These changes exhibit a complicated spatial pattern (Soomere and Räämet 2011). The mean significant wave height, H_s , evaluated using satellite altimetry data 1993–2015, varied in the range of 1–1.3 m in the Baltic proper (Kudryavtseva and Soomere 2016, 2017). This value may be slightly

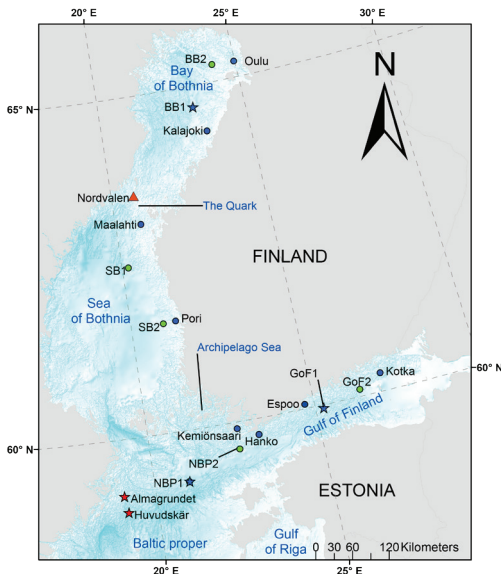


Fig 1. Map of the study area and the discussed locations. The wave measurement devices operated by the Swedish Meteorological and Hydrological Institute (SMHI) and Finnish Meteorological Institute (FMI) are marked with red and blue stars, respectively. The locations of FMI temperature buoys are shown by blue circles, WAM model grid points used in the analysis by green circles, and the south-west SMHI location Nordvalen by a red triangle.

overestimated because satellite altimetry does not recognise very low wave heights. In semi-enclosed areas like the Bay of Bothnia, the Gulf of Finland, and the Gulf of Riga, the mean H_s had lower values in the range of 0.5–1 m (Tuomi et al. 2011, Nikolkina et al. 2014).

The most disruptive storms in the Baltic Sea basin usually happen in late autumn or early winter (Suursaar et al. 2006, Björkqvist et al. 2017, 2020). The severest wave events are found in the northern part of the Baltic proper where the maximum measured H_s and peak period reached 8.2 m and over 12 s, respectively, in December 2004 (Soomere et al. 2008, Tuomi et al. 2011, Björkqvist et al. 2018). Waves can also be very high in the Sea of Bothnia; for example, in January 2019, the maximum H_s and the peak period in the southern part of this basin reached 8.1 m and 12 s, respectively (Björkqvist et al. 2020).

The long-term changes in the wind and wave properties in the Baltic Sea region are less reli-

ably known than their short-term variations. Wind speeds have increased at an 850 hPa level over the Atlantic Ocean (Pryor and Barthelmie 2003, Torralba et al. 2017) and strong westerly winds have become more frequent in the Baltic region (Ruostenoja et al. 2019). These trends, however, seem to be controversial in the Baltic Sea also in terms of wave heights (Hünicke et al. 2015, Rutgersson et al. 2022). Estimated by the satellite altimetry, the mean significant wave height H_s increased by 0.005 m yr⁻¹ from 1993 to 2015 over the Baltic Sea. This trend is more discernible in the western part of this basin (Kudryavtseva and Soomere 2017). A large part of this change is controlled by the two above-mentioned atmospheric circulation systems (Najafzadeh et al. 2021). Even though the average wave heights have increased only marginally, unexpectedly severe wave conditions have been recorded in the 21st century (Björkqvist et al. 2017, 2020). Other analyses also indicate that extremes may increase (Mäll et al. 2020) and become more frequent (Kudryavtseva et al. 2020).

The properties of waves and sea ice cover are strongly interrelated. The presence of ice affects wave growth and the generation of longer waves implicitly via reduction of the free propagation distance (Liu and Mollo-Christensen 1988) and explicitly by dissipation of wave energy (Collins et al. 2015, Mostert and Deike 2020, Tavakoli and Babanin 2021). Even though wind speeds may be even higher during the ice season, the ice cover damps wave fields and wave impact on the shore (Orviku et al. 2003, Ryabchuk et al. 2011). For example, the mean wave energy flux decreased by up to 80% due to the effects of ice in the Bohai Sea, the innermost gulf of the Yellow Sea, in winter 2011–2012 (Zhang et al. 2020).

Ice conditions in the Baltic Sea are highly variable in different years (SMHI and FIMR 1982, Haapala and Leppäranta 1996). During a mild winter, the ice extends only over the Bay of Bothnia, the Archipelago Sea, and some parts of the Gulf of Finland (Fig. 1). During an average winter, ice covers about 45% of the sea (Jevrejeva 2001). In a severe winter (e.g., in 1947), the entire sea may be covered by ice (Jevrejeva 2001, Leppäranta and Myrberg 2009,

Section 7.1). The ice season's length varies from 5 to 7 months and the ice may cover 10–100% of the total area of the Baltic Sea (Jevrejeva 2001, Leppäranta and Myrberg 2009, Section 7.2).

Sea ice and its extent are highly susceptible to rising temperature. An increase in winter air temperature by 1°C over the Baltic Sea reduces the ice season's length by 1–2 weeks and the ice-covered area by 2.5% of the basin area (Leppäranta 2012). The current climate change has led to a shorter ice season in the Arctic (Overeem *et al.* 2011) and milder (ice) winters in the Baltic Sea (Omstedt *et al.* 2004, Haapala *et al.* 2015).

The ice season duration has decreased by 10–30 days per century in the southern Baltic proper in the period 1896–1993 (Sztobryn 1994, Vihma and Haapala 2009). The ice breakup has shifted by two days per century in severe winters in the Gulf of Riga in the period 1529–1990 (Jevrejeva 2001). The changes in the ice season duration (Omstedt *et al.* 2004, Käyhkö *et al.* 2015) are slower in the northern Baltic proper or the Gulf of Finland (Haapala and Leppäranta 1997, Jevrejeva *et al.* 2004). The duration of ice season in the northern Bay of Bothnia and southern Sea of Bothnia (Fig. 1) has decreased by 18 and 47 days per century, respectively (Haapala *et al.* 2015, Section 8.3). This process is even faster in the Gulf of Finland (Sooäär and Jaagus 2007, Merkouriadi and Leppäranta 2014).

The combination of a shorter ice season and more severe wave conditions imply that, the coastlines of the Baltic Sea are systematically more exposed to the surges and waves (Omstedt and Nyberg 1996, Barnhart *et al.* 2014). This shift may cause rapid erosion or alteration in some coastal areas (Orviku *et al.* 2003, Overeem *et al.* 2011) even though the impact of ice ridges on the nearshore seabed may decrease. It is thus important to consider, at least qualitatively, the consequences of the changes to the properties of the ice season on the future of the seasonally ice-covered Baltic Sea.

Tuomi *et al.* (2011) introduced five approaches for wave statistics under such conditions. Type M statistics include only measurements (e.g., Broman *et al.* 2006). Type F only includes the data during the ice-free season that is usually normalised due to the different number of ice-free data points. Type N statistics

reflect the idealised ice-free conditions during the whole year (e.g., Suursaar and Kullas 2009). The latter approximation has been used in simulations of wave climate of the Baltic Sea using the WAM model and geostrophic winds (Räämet and Soomere 2010).

All these approaches generally introduce a systematic alteration in the established wave features (Tuomi *et al.* 2019). Type N statistics leads to an overestimation of the cumulative wave energy and energy flux. The magnitude and even the sign of the difference between estimates of mean wave properties using different approaches depend on whether the ice season is windier or calmer than the rest of the year. Björkqvist *et al.* (2018) noted that the mean H_s in the Bay of Bothnia was reduced by 30% when the ice time was included in the statistics, but the impact of ice was negligible to the south of latitude 59.5°, that is, to the south of the mid-latitude of the Gulf of Finland.

Here, we make an attempt to evaluate the potential impact of changes in the sea ice season duration on the wave statistics based on a comparison of the WAM model data during the ice-free time (Type F) and over the whole year in idealised ice-free conditions (Type N). The difference between the two estimates is used to characterise to a first approximation the impact of ice using only idealised ice-free simulations. The focus is on the potential changes in the cumulative wave energy and energy flux over certain time intervals and seasons in the northern Baltic Sea.

Specifically, we explore how the presence of seasonal ice cover impacts some widely used categories of wave statistics, how much the presence of ice reduces the wave impact compared to an idealised ice-free climate, whether this reduction has changed over the years, and at which locations the reduced ice cover in the near future may substantially modify wave-driven hydrodynamic loads.

We employ the new satellite-derived OSI-450 (Lavergne *et al.* 2019) ice concentration measurements to identify the ice season. The time series of wave height, wave energy, and wave energy flux are hindcast by the WAM model. The results are validated using available *in-situ* wave data. We start from a short descrip-

tion of data used in this study and the method of calculating wave energy flux. We then provide wave statistics and their changes introduced by the variations in the length of the ice season, and discuss which parameters influence the difference between Type F and N statistics for model and *in-situ* data, respectively. Finally, we discuss the outcome and formulate the conclusions.

Data and methods

The analysis is based on the concentration of ice cover in the Baltic Sea retrieved from satellite microwave radiometry, validated using the classic ice charts and represented in terms of the start, end and duration of the ice season for each winter at selected locations. This data set is complemented by *in situ* measured and numerically modelled time series of wave properties. The mean and cumulative (total) wave energy and wave energy flux for each year and ice season are used to characterise the potential impact of climatic changes to the ice properties on wave loads in the nearshore.

A typical ice season in the Baltic Sea starts in early winter and continues until the spring of the following year. Most of the extreme wave events and thus conditions that provide large portions of wave energy flux occur from September to February (e.g., Björkqvist *et al.* 2018). Therefore, the windiest months often overlap with the ice season in the northern Baltic Sea. For this reason, even small changes in the start or duration of the ice season may lead to considerable changes in the wave impact at some locations.

Sea ice

The sea ice concentration data used for this study are OSI-450 (Lavergne *et al.* 2019), which is the second major version of the EUMETSAT Ocean and Sea Ice Satellite Application Facility (OSI SAF) global Sea-Ice Concentration (SIC) Climate Data Record (v2.0 2017). The data provided by Norwegian and Danish Meteorological Institutes are accessible at <http://osisaf.met.no> [accessed in February 2021]. The first version of the OSI SAF SIC (OSI-409, the predecessor of

OSI-450) started in 2006. The main difference between these two datasets is a new Open Water (Weather) Filter (Gloersen and Cavalieri 1986, Buehner *et al.* 2016) which is applied on OSI-450. It removes the false sea ice over open water regions that exhibited weather-induced noise while protecting the records of low ice concentration values. Moreover, the implemented algorithms for OSI-450 are more precise (Lavergne *et al.* 2019) and new sources of satellite input data (from the EUMETSAT Climate Monitoring Satellite Application Facility) are used. A thorough description of the processes is presented in Tonboe *et al.* (2016). The detailed list of similarities and differences between the two versions is described in the product user manual (available on <http://osisaf.met.no>) [accessed in February 2021].

The global collection of sea ice concentrations, OSI-450, has daily records from 1979 to 2015 with a spatial resolution of 25×25 km. The dataset provides the ice concentration, flags, and uncertainty estimations. Ice concentration is the share of the grid area covered by ice (%). Each ice concentration value is associated with a flag and a measure of uncertainty. The flags present information about the processing steps and levels that may have an effect on the ice concentration value. The uncertainty estimation for each sea ice concentration is given as standard deviation (%). The entries with this flag equal to 0 present a nominal ice concentration value (%) which is modified for sea ice concentration and uncertainties (%). The values in the database were thoroughly checked for outliers and possibly erroneous data. To remove unreliable measurements, we only use the data with flag 0. Selecting only the data with the flag values equal to 0 drastically improved the quality of OSI-450 ice maps in the Baltic Sea region.

Following the classic notion of the duration of ice cover (e.g., Jevrejeva 2001), we use only two dates for each year: the beginning and end of the ice season. The entire time period between these dates is interpreted as the ice season. This interpretation may overlook a few days when open-sea ice has drifted to another location. However, coastal regions of the north-eastern Baltic Sea have numerous small islands, peninsulas and bays cut into the mainland. This region

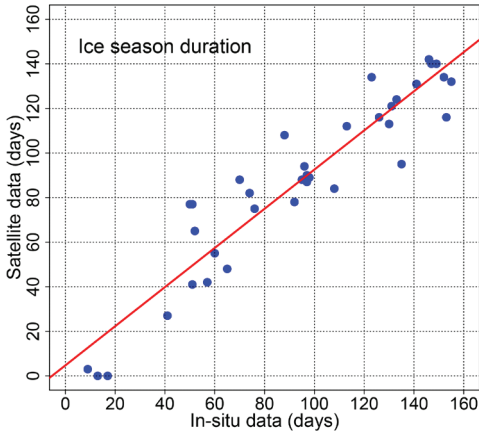


Fig 2. Satellite-derived ice season duration from OSI-450 ($\zeta = 50\%$) versus in-situ ice season duration observed at SMHI Nordvalen station. The red line represents the linear regression line.

usually has non-moving (fast) ice during the entire time period when ice is observed in the offshore. Therefore, even though this approximation may be not be exact for offshore sea areas, it apparently is adequate in terms of waves and wave energy that reaches the nearshore.

The beginning of the ice season at a particular location was estimated as the time of the first reliable measurement with the ice concentration exceeding a certain threshold, ζ , after the 1st of July. The end of the ice season is considered as the time of the last measurement with the ice concentration $> \zeta$ before the 1st of July the following year. The algorithm was implemented in the R (ver. 4.0.3) programming language (Kabacoff 2011).

To find the most suitable ice concentration cutoff ζ , the ice season duration retrieved from OSI-450 at an observation location near Storskäret in the Quark area in the waters of Maalahti municipality (referred to as Maalahti below, Fig. 1) is compared with the one derived from the Swedish Meteorological and Hydrological Institute (SMHI) ice charts for a range of cutoff values. The satellite-derived duration of the ice season is sensitive to the selected values of ζ . The best match was achieved using $\zeta = 50\%$, resulting in a correlation coefficient of 0.91 between the two estimates. The bias and root-mean-square of the two estimates are 10.53% and 21.35 days, respectively. Therefore, the ice

concentration cutoff of 50% was used in the analysis.

The satellite-derived estimates of the ice season duration obtained from OSI-450 ice data were compared with similar estimates retrieved from the SMHI ice charts. The ice season's summary observed by the SMHI since 1970, charts and reports are available at http://www.smhi.se/oceanografi/istjanst/havsis_en.php [accessed in February 2021]. This data set reflects information from SMHI ice observers, pilot stations, ice-breakers, coastguard observations, and satellite images. The ice season duration is defined as the total number of days with ice. To compare the satellite-derived ice season data with the direct ice observations, we used the data from the SMHI south-west Nordvalen (63.54°N, 20.73°E) ice observation location and its nearest OSI-450 satellite ice measurement location at 63.54°N, 20.76°E.

The estimates of the ice season duration based on SMHI observations and OSI-450 at Nordvalen showed good correspondence (Fig. 2; correlation coefficient 0.94) and almost no bias (intercept of the linear regression line at 4.7 days; slope 0.88). Three ice-free winters from OSI-450 correspond to less than 20 locally observed ice days per year. This mismatch suggests that satellite information tends to overlook small ice concentrations that are spotted by other means. This feature may also reflect relatively large intervals and gaps in the satellite data.

The further analysis uses only the properties of ice seasons retrieved using satellite information. The longest average ice season lasts about 107 days in the Bay of Bothnia (Fig. 3). This is up to two months longer than in the lower-latitude sub-basins, such as the Sea of Bothnia (Maalahti, also Storskäret, mean duration 86 days), the Gulf of Finland (GoF1, 53 days), and Kemiön-saari (Kalvören) in the Baltic proper (53 days).

Many areas in the western part of the Baltic Sea, including SMHI wave buoys and observation locations, experience ice only during average and severe winters. The satellite OSI-450 ice data rarely indicate ice in these areas and the satellite-derived ice season duration is zero in most of the years. Therefore, the effect of sea ice on wave properties and wave loads in the nearshore are generally small at such locations

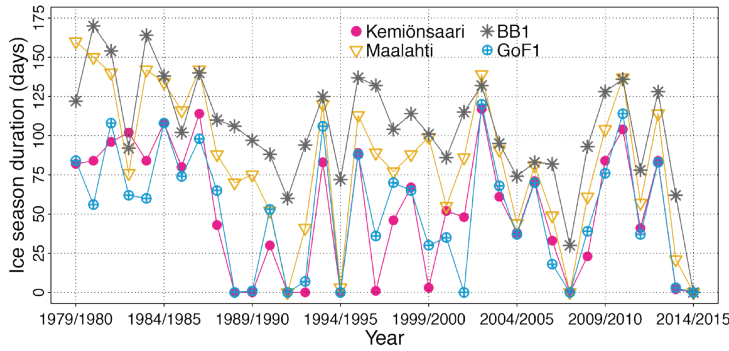


Fig 3. Ice season duration at different locations based on OSI-450 satellite data.

and apparently cannot be reliably identified from the data set used for this study.

Wave data

To select the areas where our analysis is meaningful, we calculate the percentage of years with nonzero ice season from the total number of years (27). Considering seven measurements per covariate (ice season duration and the wave statistics), at least 20 years with nonzero-ice season duration are necessary for an adequate estimate. For this reason, we only consider locations where $> 52\%$ of the years have nonzero ice season duration. Such areas are concentrated in the north-eastern part of the Baltic Sea; mostly in the Gulf of Finland, Sea of Bothnia and Gulf of Bothnia, and to lesser extent in the north-eastern Baltic proper.

We select for the analysis eight Finnish Meteorological Institute (FMI) buoy stations that have various purposes near the shores of Finland (Table 1): Oulu and Kalajoki in the Bay of Bothnia, Maalahti in the Quark area, Pori in the Sea of Bothnia, Kemiönsaari and Hanko in the northern Baltic proper and at the entrance to the Gulf of Finland, and Espoo and Kotka in the Gulf of Finland (Fig. 1). In order to reflect the difference in offshore and nearshore ice and wave properties, we include the location of the FMI wave buoy in the central Gulf of Finland (denoted GoF1 below for brevity), and a buoy in the central part of the Bay of Bothnia (BB1) (Fig. 1).

Several of the above locations are in very shallow water or located close to the shore where the modelled wave data may not necessarily

adequately reflect the real situation. To complement the analysis using more offshore locations, we add into consideration modelled wave data at another offshore location (BB2) in the Bay of Bothnia, two offshore locations (SB1 and SB2) in the Sea of Bothnia, and one location (NBP2) in the northern Baltic Proper and one (GoF2) in the Gulf of Finland (Fig. 1, Table 1). In addition, we employ wave data from two SMHI measurement locations at Almagrundet and Huvudskär, and from the FMI wave buoy in the northern Baltic proper (NBP1) for limited time periods.

The analysis in this study relies on the significant wave height H_s and peak period T_p of wave fields. Estimates of wave energy flux generally also require wave propagation direction. As this parameter is less frequently available, we only address the magnitude of wave energy flux. The main properties of the measurement locations and time series of H_s and T_p are provided in Table 1. More detailed information about these locations and devices is available, e.g., in Björkqvist *et al.* (2018), Nilsson *et al.* (2019). Datasets were retrieved through open data interfaces (<https://opendata-download-ocobs.smhi.se/>, <https://en.ilmatieteenlaitos.fi/open-data>) [accessed in August 2021].

The time resolution of the measured wave time series varies. The most frequent measurements (once in 0.5 h) exist for BB1, GoF1, and NBP1. The rest of the buoys (Table 1) provide data once an hour. The buoys have to be taken out of water for maintenance and also before the ice season to avoid damage by freezing. Therefore, the number of measurements and the coverage of the measured time series are different at each station.

We employ the time series of wave properties reconstructed for the Baltic Sea for 38 years (1970–2007) by Räämet and Soomere (2010) using the third-generation wave model WAM Cycle 4 (Komen *et al.* 1996). We use the wave properties at the nearest WAM model grid point to the locations in Table 1. The typical mismatch is 0.02° in both north-south and east-west directions.

The simulated data set with about 3 nautical miles spatial and one-hour temporal resolutions is based on the hypothetical condition of no-ice and thus represents Type N statistics. This data set has been produced using SMHI geostrophic winds with a spatial resolution of 1° and a temporal resolution of 6 h before September 1977 and 3 h after September 1977 that are adjusted for the surface wind at 10 m level by multiplying the speed by 0.6 and rotating the direction by 15° counter-clockwise (cf. Bumke and Hasse 1989).

This low spatio-temporal resolution of wind data and the simplified scheme for the construction of surface-level winds leads to a systematic underestimation of wave heights in some parts of

the Baltic Sea. The quality of the reconstructed wave properties varies spatially. They have a relatively good correlation with measured data and with the output of simulations using COSMO winds at the latitudes of the Gulf of Finland (Räämet and Soomere, 2021), whereas the match is much worse in the southern Baltic Sea. As the largest changes to wave conditions due to changes in the ice conditions have occurred in the northern Baltic Sea (Jevrejeva 2001) and we basically look at the currently occurring suppression of the wave impact caused by the presence of ice compared to the hypothetical ice-free conditions, this set of wave properties is generally suitable for our purposes.

Methods

We are interested in how much the presence of ice reduces the wave impact and how much this kind of reduction has changed over the years. Different viewpoints are possible for the analysis of interrelations between wave prop-

Table 1. Main parameters of locations used in this study. Water depth for the locations was estimated from (Seifert *et al.* 2001). All temperature buoys are MetOcean iCVP type.

Location and/or station name	Data Source	Device	Lat °N	Lon °E	Depth (m)	H_s (T_p) observations
Almagrundet	SMHI	Echosounder	59.15	19.13	29	1987–2003
Huvudskär	SMHI	Directional waverider	58.93	19.17	103	From 2001 (2010)
Bay of Bothnia 1 (BB1)	FMI	Directional waverider	64.68	23.24	74	From 2012 (2012)
Bay of Bothnia 2 (BB2)	WAM	WAM model output	65.25	24.20	12	
Northern Baltic proper 1 (NBP1)	FMI	Directional waverider	59.25	21.00	71	From 1996 (1996)
Northern Baltic proper 2 (NBP2)	WAM	WAM model output	59.60	22.60	46	
Gulf of Finland 1 (GoF1)	FMI	Directional waverider	59.96	25.24	55	From 2000 (2000)
Gulf of Finland 2 (GoF2)	WAM	WAM model output	60.10	26.40	58	
Espoo Kytö	FMI	Temperature buoy	60.06	24.72	25	
Hanko Längden	FMI	Temperature buoy	59.76	23.22	23	
Kalajoki Maakalla	FMI	Temperature buoy	64.30	23.55	12	
Kemiönsaari Kalvören	FMI	Temperature buoy	59.90	22.63	6	
Kotka Kuusenkari	FMI	Temperature buoy	60.27	27.11	8	
Maalahti Storskäret	FMI	Temperature buoy	63.11	20.82	3	
Oulu Santapankki	FMI	Temperature buoy	65.23	24.97	6	
Pori Kaijakari	FMI	Temperature buoy	61.62	21.39	6	
Sea of Bothnia 1 (SB1)	WAM	WAM model output	62.50	20.20	114	
Sea of Bothnia 2 (SB2)	WAM	WAM model output	61.60	21.00	48	
South-west Nordvalen	SMHI	Ice observations	63.54	20.73	25	
—	OSI-540	Satellite ice data	63.54	20.76	18	

erties and ice conditions, the latter expressed here in terms of the ice season duration. One way is to evaluate these ice-driven changes within a calendar year by comparison, for example, the cumulative wave energy flux to the shores in hypothetical ice-free conditions versus this flux over the ice-free season (Zaitseva-Pärnaste and Soomere 2013).

However, it is natural to consider the impact of the presence of ice on the wave field over whole ice seasons. This approach is extensively used in the analysis of changes to average and extreme water levels. Following Männikus *et al.* (2019), we call the time period from July of a certain year to the end of June of the subsequent year a stormy season. Such 12-month time periods contain the entire ice season for each winter and also the entire relatively windy autumn-winter season. As mentioned above, we employ the simplest proxy of the ice season where the wave data during its whole duration are discarded from the calculation.

The instantaneous values of the wave energy E (KJ m^{-2}) are calculated as:

$$E = \frac{\rho g H^2}{16}, \quad (1)$$

where ρ is the density of water (taken here constant 998 kg m^{-3}), g is acceleration due to gravity (9.81 m s^{-2}), H is the measured significant wave height of *in-situ* data and the hindcast H_s for modelled data. The wave energy flux P (KW m^{-1}) is calculated as (Guilou 2020):

$$P = E c_g, \quad (2)$$

$$c_g = \frac{\omega}{2k} \left(1 + \frac{2kd}{\sinh 2kd}\right). \quad (3)$$

Here, c_g is the group speed, ω is the angular wave frequency (rad s^{-1}), d is the water depth (m), $k = 2\pi/\lambda$ is the wave number, the wavelength, λ , is calculated from the general dispersion relation of water waves $\omega^2 = gk \tanh(kd)$ that is expressed as:

$$\lambda = \frac{gT^2}{2\pi} \tanh\left(\frac{2\pi d}{\lambda}\right). \quad (4)$$

As the energy period is often not available, T is interpreted here as the peak period. The wavelength is estimated for the approximate water depth d at each station.

The mean significant wave height $\overline{H_{sy}}$, wave energy $\overline{E_y}$ and wave energy flux $\overline{P_y}$ during a particular stormy season are calculated in a classic (Type F) manner; for example, the mean wave energy $\overline{E_y}$ in a particular stormy season is

$$\overline{E_y} = \frac{1}{N_y} \sum_{\text{year}} E_i, \quad (5)$$

where E_i is the instantaneous wave energy and N_y is the number of available measurements or modelled values of wave energy in this stormy season. Note that these estimates do not contain any information about the ice season duration. This information is reflected by the ratio of N_y and the total number of measurement instants or modelled data points during the entire stormy season.

The total (or cumulative) wave energy and especially energy flux are richer in content measures of the impact of ice cover on hydrodynamic loads in the nearshore. The wave energy goes as squared wave height and the wave energy flux in shallow water as wave energy to the power of 2.5. For example, the total stormy season wave energy flux P_{tot} was calculated as a sum of instantaneous values of energy flux P_i calculated once an hour during the two subsequent half-years (stormy season):

$$P_{\text{tot}} = \sum_{\text{year}} P_i. \quad (6)$$

The cumulative wave energy P_{tot} is calculated similarly to Eq. (6). As the time series of modelled wave data (1970–2007) and ice information in OSI-450 (from 1979) cover different time periods, we use in comparisons mostly the overlapping part of these data sets, that is, 27 stormy seasons from 1979/1980 to 2006/2007.

Results

Wave statistics during ice-free time (Type F)

We start from the analysis of temporal and spatial variability of the main wave properties in the selected locations over 27 stormy seasons (1979/1980–2006/2007). The annual mean H_s during the ice-free time of single stormy seasons (Type F statistics) for the selected stations (Fig. 4) varies by a factor of two at the study sites. The Bay of Bothnia, Oulu, with the longest ice season, is characterised by the lowest range of the mean H_s in single stormy seasons (0.38–0.55 m). This feature apparently reflects the combination of a relatively sheltered location of the particular site and well-known seasonality of wind patterns in the Baltic Sea region. Namely, the ice-free time in this part of the Baltic Sea usually matches the spring and summer seasons that have the lowest wind speed. The mean H_s in single stormy seasons at three other stations in this subbasin (BB1, BB2, and Kalajoki) varied between 0.50 m and 0.77 m. Both these locations (BB1, Kalajoki) are open to the predominant moderate and strong south-western winds in this region. The somewhat larger mean H_s at BB1 (0.72 m) evidently reflects its more open position compared to Kalajoki.

Stations in the Sea of Bothnia have a higher mean H_s (0.51–1.01 m) and shorter ice season duration than in the Bay of Bothnia. It is natural that the mean H_s is higher at the offshore locations SB1 and SB2 than in more sheltered nearshore locations at Maalahti and Pori.

Kemiönsaari, on the north-eastern shore of the Baltic proper, has the second-lowest mean H_s (0.46–0.62 m). This feature might also be due to the station's location, which is sheltered against westerly winds by islands in the Archipelago Sea (Fig. 1). The Hanko station is located to the south of Kemiönsaari. It is open to the predominant moderate and strong westerly winds over the Baltic proper and has higher mean H_s values (0.54–0.77 m). As expected, the much more open location in the northern Baltic proper (NBP2) has clearly higher mean H_s values than those hindcast for Kemiönsaari or Hanko.

In the Gulf of Finland, the GoF1 wave buoy in the central Gulf of Finland has a higher mean H_s (0.55–0.87 m) compared to similar estimates for Espoo, GoF2, and Kotka (0.44–0.73 m). Generally, the farther the station is located from the coast, the higher is the mean H_s at this station. This feature becomes evident in each subbasin, except for the GoF2 location. The calculated values of mean H_s are consistent with the results provided by Björkqvist *et al.* (2018), who estimate the ice-free (Type F) mean H_s for the Baltic Sea from a 41-year SWAN model hindcast. It can be therefore concluded that variations in the ice season duration have a clearly smaller impact on Type F statistics of mean wave properties than the location of the particular site.

The boxplots of magnitude and scatter of other mean Type F properties of wave fields (not shown) evaluated using the WAM model are similar to those presented in Fig. 4. As expected, the stormy season mean of wave energy during ice-free time (Fig. 5) calculated using Eq. (5) has much larger interannual and spatial variation than the mean H_s . Its magnitude varies by a factor of up to 3 at all locations in 1979/1980–2006/2007. The mean wave energy over all the years also varies by a factor of 3 at different stations. It reaches a maximum of 0.79 KJ m⁻² at GoF1, is less than ~0.71 KJ m⁻² at BB1 and mostly between 0.2 and 0.3 KJ m⁻² at Kemiönsaari.

Both interannual and spatial variations in the ice-free (Type F) mean wave energy flux (Fig. 6) are, as expected, even larger than similar variations in the wave energy (Fig. 5). The long-term mean of this quantity varies from about 1 KW m⁻¹ at Kemiönsaari up to 2.5 KW m⁻¹ at Maalahti, BB1 and GoF1. This level is almost the same as the relevant Type N values for nearshore areas of the western Baltic proper (Soomere and Eelsalu 2014). A natural reason for relatively large wave energy flux at the sites in question is that they are located at a larger distance from the shore and in deeper areas than the "converter line" locations addressed by Soomere and Eelsalu (2014). The patterns of interannual variations in the mean energy and energy flux (Figs. 5 and 6) are almost identical at all locations. This feature indicates that wave periods in the storms that provide the largest contribution

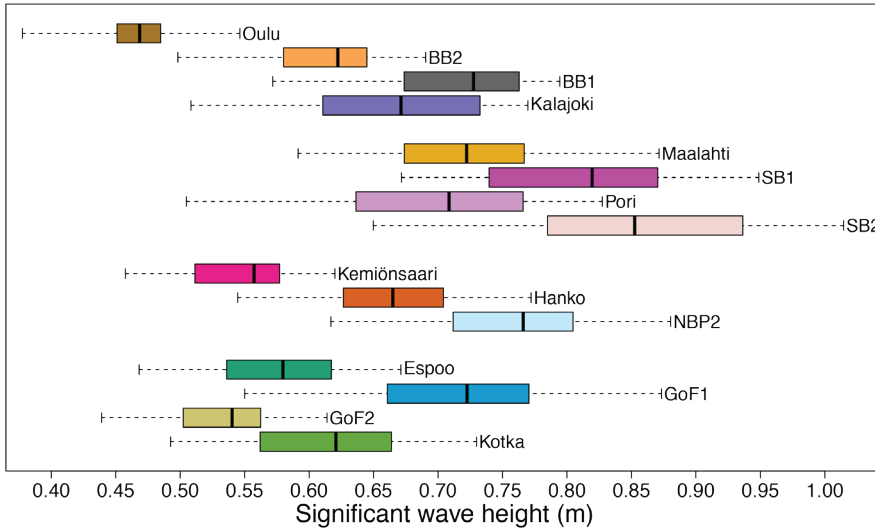


Fig 4. Boxplot of ice-free modelled mean H_s (Type F statistics) during 27 stormy seasons from 1979/1980 to 2006/2007. The coloured area reflects the two middle quartiles of stormy season mean H_s . The vertical line in this area represents the median H_s (in terms of mean H_s in single stormy seasons). The sections denoted by dashed lines represent the lowest and the highest quartiles. The maximum and minimum H_s at the particular location are shown using small vertical lines.

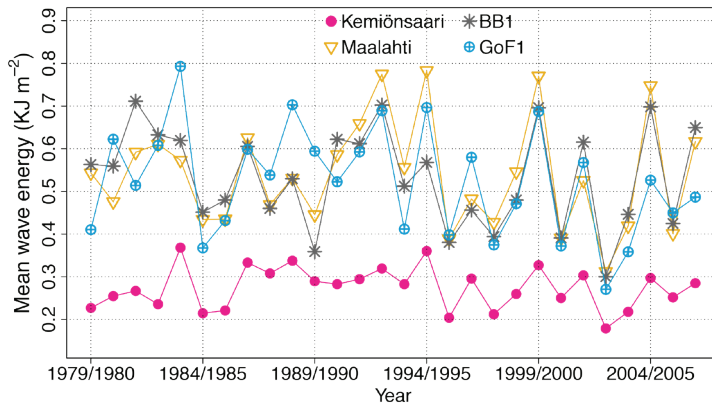


Fig 5. Mean ice-free wave energy (Type F statistics) evaluated from the WAM model output during stormy seasons 1979/1980–2006/2007.

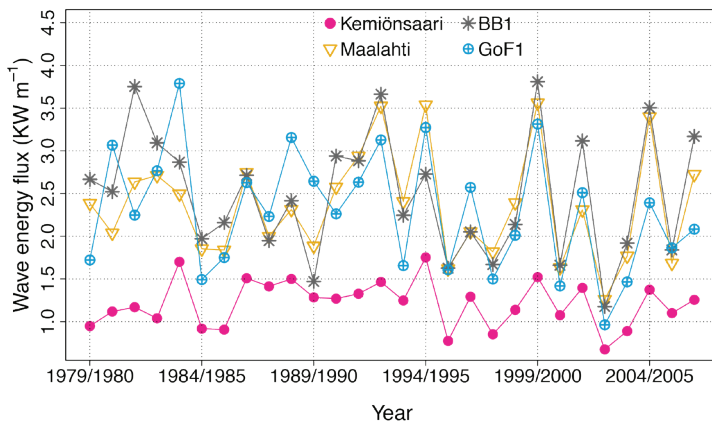


Fig 6. Mean ice-free wave energy flux (Type F) evaluated from the WAM model output during stormy seasons 1979/1980–2006/2007.

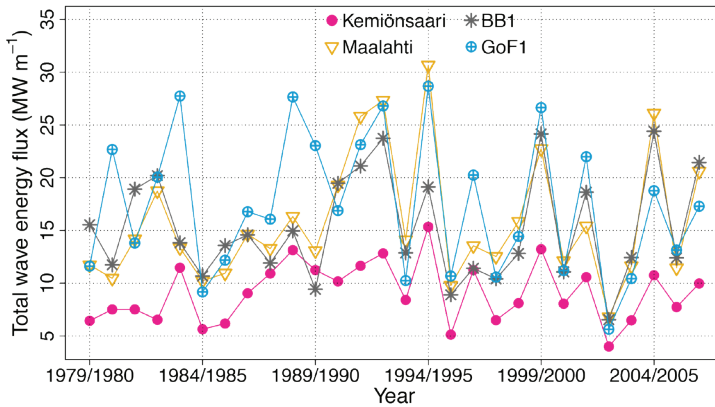


Fig 7. Mean ice-free total (cumulative) wave energy flux (Type F) evaluated from the WAM model output during stormy seasons 1979/1980–2006/2007.

to the wave energy flux vary insignificantly. This conjecture is consistent with the perception that severe wave fields in the study area are generally fetch-limited.

Spatio-temporal variations in the cumulative Type F properties of wave fields at the locations in question are even larger. For example, the cumulative wave energy flux P_{tot} at GoF1 varies almost by a factor of 6 in individual stormy seasons (Fig. 7). This feature indicates that intermittency of wave properties is evident not only between single storms and seasons (Soomere and Eelsalu 2014) but also in terms of different years.

Interestingly, spatial differences in this quantity at separate locations are smaller than similar differences for wave energy or energy flux. The mean P_{tot} varies only by a factor of 2 at locations represented in Fig. 7. In the light of the normally fetch-limited nature of the Baltic Sea wave fields (that suppresses differences in wave periods under severe wave conditions), this feature may indicate that the strongest wave storms that provide a very large contribution to the total wave energy flux (Soomere and Eelsalu 2014) impact simultaneously all considered locations and occur before the ice season starts even at the northernmost locations.

To validate the described ice-free wave statistics to some extent, we compared wave statistics derived from *in-situ* measurements (Type M; Tuomi *et al.* 2011) with similar statistics obtained from wave simulations. The beginning and the end of the ice season were estimated from the satellite observations as described

above. Wave buoys are removed before the ice season starts. Thus, in the northern part of the Baltic Sea, the measurement period is typically from May/early June until December/early January (Tuomi *et al.* 2019), and only a few locations and years are suitable for such a comparison. Some buoy measurements have been made with ice concentration up to 40%, according to satellite data, which possibly indicates an invalid interpretation of satellite information. The only station in the study area that experiences frequent and long ice cover with an overlap of more than 5 years of our model data and the measurements is at GoF1. Simultaneous observations and model data are available during the period 2001/2002–2006/2007. Based on OSI-450 ice data, the ice season duration varied in the range of 0–120 days during these years (Fig. 3). The wave properties during the ice-free time, based on simulations (Type F) and *in-situ* (Type M) data, considerably varied during these years, showing the difference in wave energy flux in the range of 3% to 48% (in 2002/2003, which has the longest ice season, 120 days).

The difference is even larger for single stormy seasons at locations in BB1 that allow a comparison of this kind. At Almagrundet the difference in the wave energy flux P_{tot} is 62% with 22 days of ice for 1994/1995. Huvudskär and the FMI buoy (NBPI) location in the northern Baltic proper have wave measurements in 2002/2003 with 12 and 34 day ice season duration, respectively. The difference between Type F and M wave energy flux is 47% and 34%, respectively, at these locations. This estimate of the difference

between the ice-free (Type F) and the measurement statistics (Type M) matches a similar estimate by Björkqvist *et al.* (2018) for the Bay of Bothnia and apparently characterises years with long and extensive ice cover in the northern Baltic Proper.

Impact of the presence of ice on mean wave properties

A first-order perception of the impact of the presence of ice cover on wave properties can be inferred from a comparison of the box and scatter plots of the difference in modelled wave properties that reflect statistics Type F and N. The relevant quantities characterise to some extent the impact of the presence of ice in the current climate against a hypothetical ice-free climate that has the same wind regime as the climate today. The magnitude of this difference exemplifies, to a first approximation, changes to hydrodynamic loads that could be expected in a much warmer climate. The addressed properties (mean H_s , mean and cumulative wave energy and energy flux) for stormy seasons from 1979/1980 to 2006/2007 show the impact of ice from different viewpoints.

The difference in H_s calculated for the selected stations in each subbasin (Fig. 8) first of all indicates that the mean H_s in totally ice-free conditions would generally exceed that in the current climate. The only exception is Pori, where the evaluated difference is -0.25% . Virtually no changes are projected at SB1, SB2, Kemiönsaari, Hanko, Espoo, GoF1 and GoF2. The ice season is relatively short at these locations and the sites are open to the predominant strong wind directions (Fig. 1). At locations with longer ice season duration, the completely ice-free wave regime would lead to an increase by 3–5% in the mean H_s . The largest increase ($> 10\%$) is projected to the locations at higher latitudes, such as Oulu in the Bay of Bothnia. The rate of increase in the mean H_s in single stormy seasons could be much larger, up to 28% at Oulu. Kalajoki and BB1, with the longest ice season duration after Oulu, also host very large rates of increase in the stormy season mean H_s , 24% and 23%, respectively. Interestingly, on many occasions, the mean single stormy season

H_s may decrease in the completely ice-free statistics. As mentioned above, this feature apparently reflects the (mis)match of the relatively windy season with the ice season.

The situation is generally the same with the stormy season mean wave energy and energy flux (Figs. 9 and 10). The impact of the presence of ice on these quantities is negligible at Pori, somewhat unexpectedly in the offshore of the Sea of Bothnia (at SB1 and SB2) and generally at all locations where the ice season is relatively short. The magnitude of this impact increases towards the North and East. This gradient matches the increase in the ice season duration. The impact of ice is, as expected, the largest in the Bay of Bothnia, especially in the coastal area (Oulu), where the mean wave energy in the ice-free climate may be 20% larger than now.

The difference between the increase rates for mean wave energy (Fig. 9) and energy flux (Fig. 10) is just a few per cent. Therefore, the existing Type F estimates of annual mean wave energy and energy flux adequately (within a few per cent) represent also the hypothetical ice-free situation in the northern Baltic Sea, except in the Bay of Bothnia and the eastern Gulf of Finland, where the difference may reach 20% for wave energy and almost 30% for the wave energy flux. Interestingly, the pattern of differences is asymmetric: large positive differences (equivalently, underestimation of mean wave energy in Type N statistics) are more likely than large negative differences.

The difference between Type F and N statistics for energy in single stormy seasons is much larger, up to 54% (Fig. 9) at Oulu. This feature suggests that the shift to completely ice-free conditions in a future climate will probably lead to large changes in the wave energy and energy flux in single stormy seasons, but the mean wave properties are represented adequately by Type F statistics in most of the Baltic Sea as indicated also by Björkqvist *et al.* (2018).

Impact of the presence of ice on cumulative wave statistics

The impact of sea ice on cumulative properties of the wave climate is much larger compared to

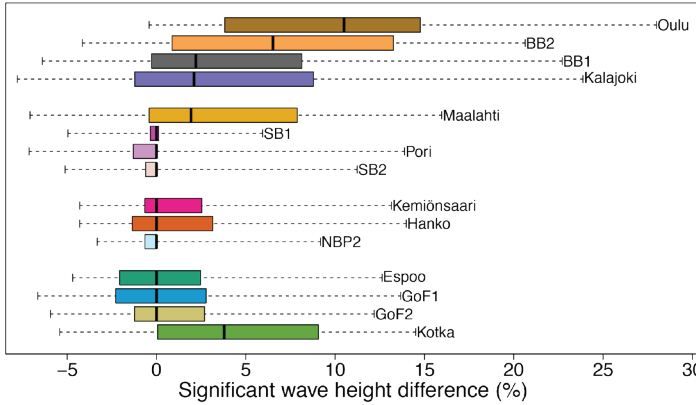


Fig 8. The difference of Type F and N estimates of mean H_s in single stormy seasons.

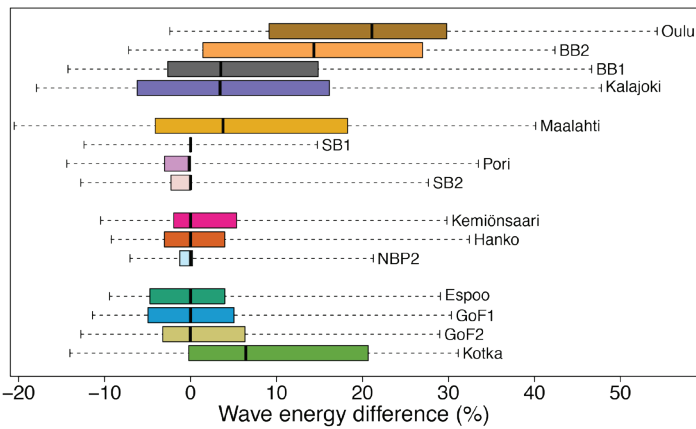


Fig 9. The difference of Type F and N estimates of mean wave energy in single stormy seasons.

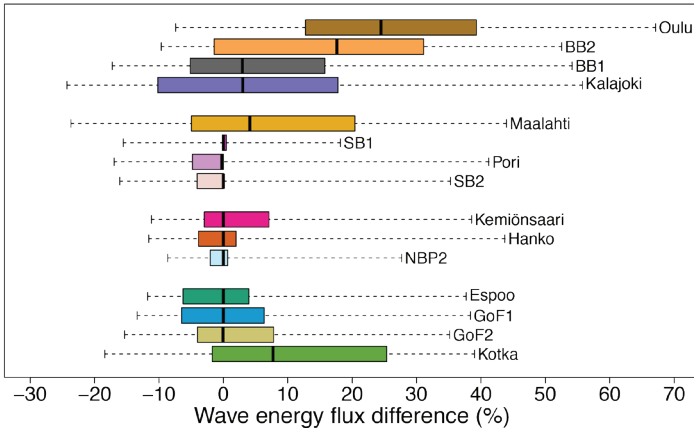


Fig 10. The difference of Type F and N estimates of mean wave energy flux in single stormy seasons.

the above. Its magnitude at a particular site obviously depends on the ice season duration and the least (zero) difference characterises the years with no ice.

The largest mean difference of cumulative wave energy E_{tot} (Fig. 11) between Type F and Type N estimates is 57% at Oulu where and it can reach up to 82% in a single stormy season.

For other locations in the Bay of Bothnia it reaches about 47% for BB2 and 37% for BB1 and Kalajoki, which are the largest values for differences in E_{tot} among the considered subbasins.

Although the ice season is shorter in the northern Baltic proper and Gulf of Finland than in the Sea of Bothnia, the existence of ice leads to a decrease in the E_{tot} by up to 59% in

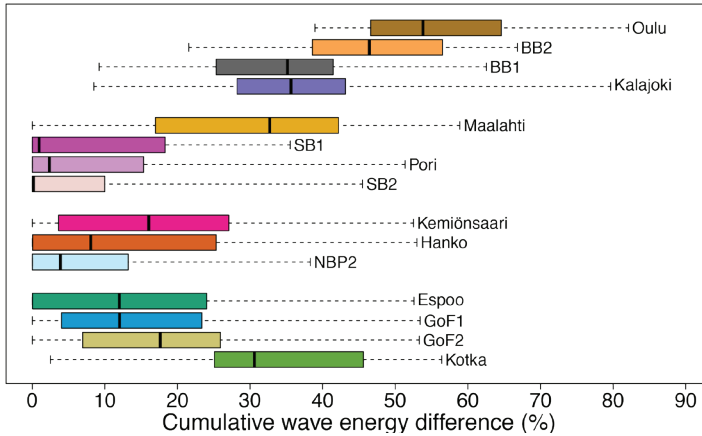


Fig 11. The difference of Type F and N estimates of cumulative wave energy in single stormy seasons from 1979/1980 to 2006/2007.

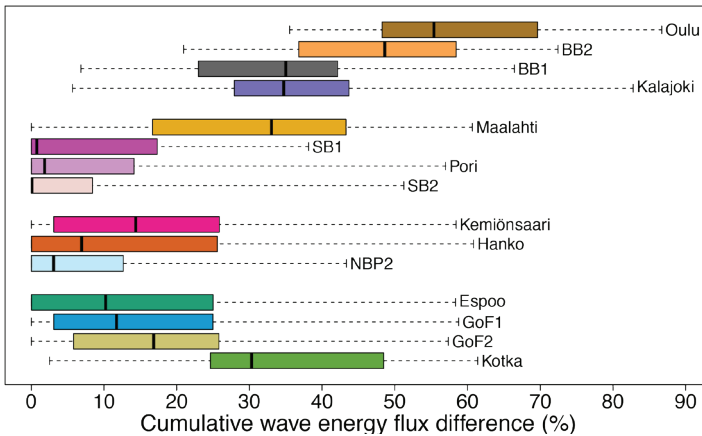


Fig 12. The difference of Type F and N estimates of cumulative wave energy flux in single stormy seasons.

single stormy seasons (Fig. 11). Interestingly, the decrease in this quantity is relatively small, below 15% on average, at several locations of the Sea of Bothnia and the Gulf of Finland. The ice-driven decrease in E_{tot} is smallest (8.5%) at SB1 in the Sea of Bothnia.

The patterns of differences between Type F and Type N statistics for cumulative wave energy flux P_{tot} (Fig. 12) insignificantly (usually no more than by a few per cent) differ from those evaluated for cumulative wave energy E_{tot} . This small difference in the estimates in Figs. 11 and 12 again indicates that wave periods (and thus group velocities) in strong storms mostly depend on the fetch length and less on the wind speed.

The above has shown that Type F statistics gives on most occasions an adequate estimate of mean wave properties in the idealised ice-free climate. However, quantities based on cumulative wave properties substantially underestimate

the total wave energy and especially energy flux to the coastal areas. It is thus essential to consider the ice season's duration when using wave statistics in coastal or other applications where cumulative properties of waves are decisive.

Wave statistics and ice season duration

The natural dependence of cumulative properties of wave fields on the presence of sea ice obviously reflects the different number of modelled (or measured) snapshots of wave properties during the ice-free time and during the entire year or stormy season. The longer the ice season, the fewer wave measurements are included in the Type F statistics. However, the interrelations between the number of wave data entries and the mean H_s , wave energy and energy flux are not straightforward.

The mean ice season duration at the considered locations (Table 1) varies from 25 (SB2) to 167 (Oulu) days. A scatter diagram of ice season duration and mean wave height at four locations (Fig. 13) shows that a longer ice season duration generally corresponds to a lower value of stormy season H_s . In other words, interannual variations in the wave energy are in counter-phase with the ice season duration. The mean H_s decreases when the ice season becomes longer at all considered locations (Table 2) even though at some locations (e.g., BB1, Fig. 13) the slope of the relevant trend is very small. This decrease is statistically significant at a 99% level at five locations in or at the entrance of the Gulf of Finland: Espoo, Hanko, Kemiönsaari, Kotka and central Gulf of Finland (GoF1).

Compared with Kemiönsaari, the correlation between these two parameters is much weaker at Maalahti (the mean ice season duration 1979–2007 is 90 days), Oulu and Pori. No correlation exists at BB1 (where the mean ice season duration is 110 days) and Kalajoki. The spatial pattern of similar correlation coefficients between the ice season duration, wave energy and energy flux for ice-free time is almost the same (Table 2). The values of correlation coefficients are also almost the same for H_s , wave

energy and energy flux. The correlation coefficient between the ice season duration and the wave energy at Espoo, Hanko, Kemiönsaari, Kotka, and GoF1 reveal a statistically significant negative correlation at a > 99% confidence level (Table 2). Only at Oulu are these correlations for energy and energy flux clearly stronger than the correlation for H_s . A similar pattern of interrelations becomes evident for the ice season duration and mean wave energy flux (Fig. 14).

The presence of ice at these five locations in and near the Gulf of Finland, therefore, impacts not only the cumulative quantities but also the addressed mean properties of wave fields. The above has shown that, somewhat unexpectedly, the existing Type F statistics would remain correct also in some future ice-free climates. However, not unexpectedly, at the latitudes of the Gulf of Finland some properties of Type F statistics of the idealised ice-free wave climate apparently will differ from the similar properties of the current wave climate.

As spring is relatively calm in the study area, the presented material indicates that the time instant of ice formation at the latitudes of the Gulf of Finland often falls into the middle of a relatively windy winter. Derived from satellite data, the ice season at these latitudes typically

Table 2. Pearson correlation coefficients and relevant p -values between ice season duration and mean H_s , wave energy (E) and wave energy flux (P) for the ice-free season. Locations with p -values indicating statistical significance of the correlation at a > 99% level are shown with bold font. Note that adjusted R^2 may take small negative values.

Location	Ice season duration vs. H_s			Ice season duration vs. E			Ice season duration vs. P		
	Correlation	Adj. R^2	p	Correlation	Adj. R^2	p	Correlation	Adj. R^2	p
Espoo	-0.63±0.12	0.37	0.00	-0.62±0.12	0.36	0.00	-0.60±0.13	0.33	0.00
Hanko	-0.66±0.11	0.42	0.00	-0.64±0.12	0.39	0.00	-0.61±0.12	0.34	0.00
Kalajoki	-0.19±0.18	-0.00	0.33	-0.16±0.18	-0.01	0.42	-0.16±0.18	-0.01	0.41
Kemiönsaari	-0.59±0.13	0.32	0.00	-0.55±0.14	0.27	0.00	-0.54±0.14	0.27	0.00
Kotka	-0.54±0.14	0.27	0.00	-0.55±0.13	0.28	0.00	-0.55±0.14	0.27	0.00
Maalahti	-0.43±0.16	0.16	0.02	-0.44±0.16	0.16	0.02	-0.43±0.16	0.16	0.02
Oulu	-0.37±0.16	0.10	0.05	-0.43±0.16	0.16	0.02	-0.46±0.15	0.18	0.01
BB1	-0.08±0.19	-0.03	0.69	-0.09±0.18	-0.03	0.65	-0.11±0.18	-0.03	0.58
BB2	-0.35±0.17	0.09	0.07	-0.29±0.17	0.05	0.13	-0.26±0.18	0.03	0.17
Pori	-0.31±0.17	0.07	0.09	-0.28±0.17	0.04	0.15	-0.27±0.17	0.04	0.16
GoF1	-0.62±0.12	0.36	0.00	-0.61±0.12	0.34	0.00	-0.59±0.13	0.32	0.00
GoF2	-0.53±0.14	0.25	0.00	-0.50±0.15	0.22	0.00	-0.44±0.15	0.16	0.02
NBP2	-0.53±0.14	0.26	0.00	-0.51±0.14	0.23	0.00	-0.48±0.15	0.20	0.00
SB1	-0.32±0.17	0.07	0.09	-0.35±0.17	0.09	0.07	-0.34±0.17	0.08	0.07
SB2	-0.36±0.16	0.10	0.06	-0.33±0.17	0.07	0.09	-0.30±0.17	0.06	0.12

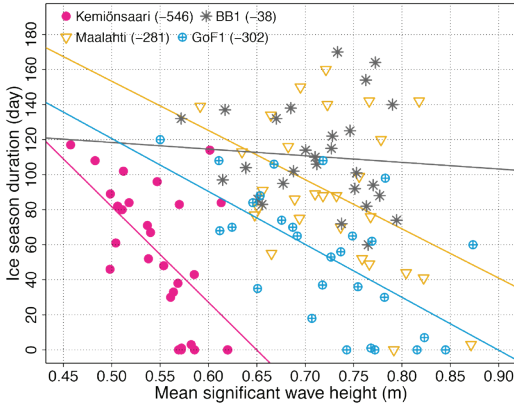


Fig 13. Scatter diagram of ice season duration and mean H_s during ice-free times at four locations of Fig. 1. The slopes of the relevant regression lines are presented in the legend.

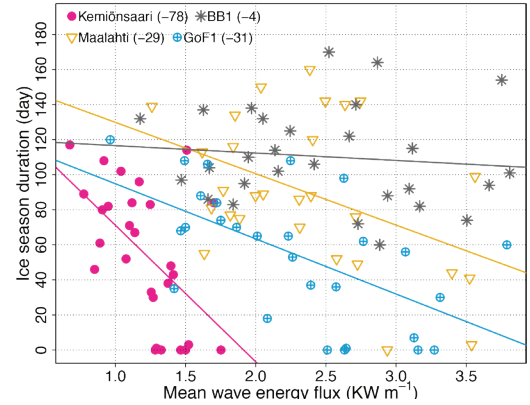


Fig 14. Scatter diagram of ice season duration and mean wave energy flux during ice-free times at four locations of Fig. 1. The slopes of the relevant regression lines are presented in the legend.

starts at the beginning of February. The formation of ice in the Sea of Bothnia and Bay of Bothnia occurs one or two months earlier, at the beginning of January and December, respectively. Therefore a large proportion of strong winds that are frequent in winter overlap with the ice season. These features together suggest that the regions of the Baltic Sea that have a relatively short ice season (especially those on the northern shore of the Gulf of Finland) may be even more sensitive with respect to changes in ice conditions under current climate change than locations in the far North where ice season lasts 3–4 months. With a longer perspective, however, a similar sensitivity will appear for the locations in the Sea of Bothnia and Bay of Bothnia.

Discussion

The main purpose of this research was to estimate how the presence of seasonal ice cover impacts the widely used categories of wave statistics, such as mean significant wave height, mean and cumulative wave energy and energy flux in the northern Baltic Sea. Specifically, we are interested in how much the presence of ice reduces the wave impact compared to an idealised ice-free climate and whether this reduction has changed over the years. An associated task was to understand whether and/or in which loca-

tions the reduced ice cover in the near future may substantially modify wave-driven hydrodynamic loads in the coastal zone. The research has been mostly performed using simulated wave data for 1970–2007 and satellite information about ice conditions since 1979. The analysis is focused on nearshore areas of the north-eastern Baltic Sea that are commonly ice-covered in winter.

The extensive variation in ice conditions and in the length of ice season in both time and space, as well as the overall shortening of the ice season in the Baltic Sea (Fig. 3), are extensively described in detail in the literature (e.g., Granskog *et al.* 2006, Omstedt *et al.* 2014, Käyhkö *et al.* 2015). Our analysis replicates this spatio-temporal variability in both mean and cumulative wave properties. It is somewhat counter-intuitive that the common statistical properties derived from idealised completely ice-free conditions (Type N) match well with similar properties evaluated for actual ice-free time (Type F) in the north of the study area. The difference in the listed mean properties of wave fields is negligible ($< 1\%$) at half the locations. It reaches the level of 2–4% in the northern Gulf of Bothnia and in the eastern Gulf of Finland, and up to 10% for energy and 20% for energy flux in the far North.

This invariance of these statistical properties of wave fields on the presence of sea ice apparently reflects a specific match of the windy and

ice seasons in the study area. The ice season starts in the relatively windy late autumn and early winter and ends in a relatively calm spring season. The described feature may be explained as a balance between statistical properties of waves during ice-free times and properties of hypothetical waves during the ice season.

It is natural that the cumulative energy and energy flux greatly depend on the presence of sea ice. These quantities grow rapidly when the ice season becomes shorter. The potential climate change driven variations in ice conditions alone may thus lead to an increase by 30–50% of the wave energy and energy flux and thus to a substantial escalation of the hydrodynamic loads in the nearshore of the study area in a long-term. An almost trivial conjecture is that the longer the ice season is today, the larger is the potential impact of sea waves in a hypothetical ice-free future climate.

A different picture becomes evident for a part of the study area. The mean wave properties are almost uncorrelated with the ice season duration in the northern part of the study area, in the Sea of Bothnia and the Bay of Bothnia. There is, however, a statistically significant correlation (at a > 99% level) of these quantities at the latitudes of the Gulf of Finland. A decrease in the ice season duration is associated with a rapid increase in the mean wave properties in this region. The rate of this rise is almost the same for mean wave height, energy and energy flux.

This established correlation reiterates the results of Zaitseva-Pärnaste and Soomere (2013), where the modelled data at three locations in the eastern Baltic Sea showed a similar negative correlation. Our analysis shed further light on this property and revealed large spatial variations of this feature in different parts of the Baltic Sea.

This spatial variability suggests that recent changes in ice conditions may lead to a radically distinct reaction of wave properties and impacted coastal areas in different regions. The invariance of mean wave parameters on the ice season duration in the northern part of the study area suggests that climate warming and the associated loss of sea ice will have a limited impact on the mean wave properties and even on wave-driven loads in the near future at the scale of a few years to a few decades. This seems to

be the situation in the middle and northern part of the Sea of Bothnia and in the Bay of Bothnia. We note that this conjecture only applies to the changes in wave conditions in a hypothetical future climate that has the wind climate of today.

On the contrary, locations at the latitudes of the Gulf of Finland may be greatly affected also at time scales of a few years, should the ice season continue to shorten at the existing pace. A simple explanation is that at these locations the ice is formed somewhere in the middle of the relatively windy season. Any delay in the ice formation time would thus open the likelihood of more wave energy impacting the coastal area. This shift will eventually be associated with increased water levels compared to the circumstances with ice cover. If such situations are frequent, high waves will attack unprotected and unfrozen sediment on the upper parts of the beaches for much longer times and eventually cause massive coastal erosion and fine sediment relocation (Orviku *et al.* 2003, Overeem *et al.* 2011, Ryabchuk *et al.* 2011).

Conclusions

Mean properties of wave fields (significant wave height, wave energy, energy flux) in the seasonally ice-covered northern Baltic Sea can be passably estimated using hypothetical completely ice-free models while similar cumulative properties of the wave climate are overestimated by up to 82% for wave energy and 87% for wave energy flux.

The mean wave properties are almost uncorrelated with the ice season duration in the Sea of Bothnia and the Bay of Bothnia but have a statistically significant (at a > 99% level) negative correlation with the ice season duration at the latitudes of the Gulf of Finland. In other words, the longer the ice season, the lower is the mean wave height in the Gulf of Finland and adjacent areas. Another reflection of this feature is that the interannual variations in wave energy are in counter-phase with the ice season duration.

Recent climate change driven variations in the ice cover duration are unlikely to significantly impact hydrodynamic loads on the nearshore in the Sea of Bothnia and the Gulf

of Bothnia in the near future. However, these changes may considerably add energy to coastal processes at the latitudes of the Gulf of Finland.

Acknowledgements: The research was co-supported by the Estonian Research Council (grant PRG1129) and the European Economic Area (EEA) Financial Mechanism 2014–2021 Baltic Research Programme (grant EMP480). We thank the Radar Altimeter Database System (RADS), Finnish, Swedish, Norwegian and Danish Meteorological Institutes database and NOAA Center for Weather and Climate Prediction for providing the data, and Prof Kevin Parnell for suggestions towards improvement of the manuscript.

References

- Barnhart K.R., Overeem I. & Anderson R.S. 2014. The effect of changing sea ice on the physical vulnerability of Arctic coasts. *Cryosphere* 8(5): 1777–1799, doi: 10.5194/tc-8-1777-2014.
- Björkqvist J.-V., Tuomi L., Tollman N., Kangas A., Pettersson H., Marjamaa R., Jokinen H. & Fortelius C. 2017. Brief communication: Characteristic properties of extreme wave events observed in the northern Baltic Proper, Baltic Sea. *Nat. Hazards Earth Syst. Sci.* 17(9): 1653–1658, doi: 10.5194/nhess-17-1653-2017.
- Björkqvist J.-V., Lukas I., Alari V., van Vledder G. P., Hulst S., Pettersson H., Behrens A. & Männik A. 2018. Comparing a 41-year model hindcast with decades of wave measurements from the Baltic Sea. *Ocean Eng.* 152: 57–71, doi: 10.1016/j.oceaneng.2018.01.048.
- Björkqvist J.-V., Rikka S., Alari V., Männik A., Tuomi L. & Pettersson H. 2020. Wave height return periods from combined measurement-model data: a Baltic Sea case study. *Nat. Hazards Earth Syst. Sci.* 20(12): 3593–3609, doi: 10.5194/nhess-20-3593-2020.
- Broman B., Hammarklint T., Rannat K., Soomere T. & Valdmann A. 2006. Trends and extremes of wave fields in the north-eastern part of the Baltic Proper. *Oceanologia* 48(S): 165–184.
- Buehner M., Caya A., Carrieres T. & Pogson L. 2016. Assimilation of SSMIS and ASCAT data and the replacement of highly uncertain estimates in the Environment Canada Regional Ice Prediction System. *Q. J. R. Meteorol. Soc.* 142(695): 562–573, doi:10.1002/qj.2408.
- Bumke K. & Hasse L. 1989. An analysis scheme for determination of true surface winds at sea from ship synoptic wind and pressure observations. In: Munn R. E. (ed.), *Boundary Layer Studies and Applications*, Springer, Dordrecht, pp. 295–308, doi: 10.1007/978-94-009-0975-5_18.
- Collins III C.O., Rogers W.E., Marchenko A. & Babanin A.V. 2015. In situ measurements of an energetic wave event in the Arctic marginal ice zone. *Geophys. Res. Lett.* 42(6): 1863–1870, doi: 10.1002/2015GL063063.
- [EUMETSAT] 2017. EUMETSAT Ocean and Sea Ice Satellite Application Facility. *Global sea ice concentration climate data record 1979–2015* (v2.0, 2017), [Online]. Norwegian and Danish Meteorological Institutes, doi: 10.15770/EUM_SAF_OSI_0008.
- Gloersen P. & Cavalieri D.J. 1986. Reduction of weather effects in the calculation of sea ice concentration from microwave radiances. *J. Geophys. Res.-Oceans* 91(C3): 3913–3919, doi: 10.1029/JC091iC03p03913.
- Goerlandt F., Montewka J., Zhang W. & Kujala P. 2017. An analysis of ship escort and convoy operations in ice conditions. *Saf. Sci.* 95: 198–209, doi: 10.1016/j.ssci.2016.01.004.
- Granskog M., Kaartokallio H., Kuosa H., Thomas D. N. & Vainio J. 2006. Sea ice in the Baltic Sea – A review. *Estuar. Coast. Shelf Sci.* 70(1–2): 145–160, doi: 10.1016/j.ecss.2006.06.001.
- Guillou N. 2020. Estimating wave energy flux from significant wave height and peak period. *Renew. Energy* 155: 1383–1393, doi:10.1016/j.renene.2020.03.124.
- Haapala J. & Leppäranta M. 1996. Simulating the Baltic Sea ice season with a coupled ice-ocean model. *Tellus A* 48(5): 622–643, doi:10.3402/tellusa.v48i5.12158.
- Haapala J. & Leppäranta M. 1997. The Baltic Sea ice season in changing climate. *Boreal Environ. Res.* 2(1): 93–108.
- Haapala J.J., Ronkainen I., Schmelzer N. & Sztobryn M. 2015. Recent change–sea ice. In: The BACC II Author Team, *Second Assessment of Climate Change for the Baltic Sea Basin*, Regional Climate Studies, Springer, Cham, pp. 145–153, doi: 10.1007/978-3-319-16006-1_8.
- Harff J., Deng J., Dudzińska-Nowak J., Fröhle P., Groh A., Hünicke B., Soomere T. & Zhang W. 2017. What determines the change of coastlines in the Baltic Sea? In: Harff J., Furmańczyk K., von Storch H. (eds.), *Coastline Changes of the Baltic Sea from South to East*, Springer, Cham, pp. 15–35, doi: 10.1007/978-3-319-49894-2_2.
- Hünicke B., Zorita E., Soomere T., Madsen K.S., Johansson M. & Suursaar Ü. 2015. Recent change–sea level and wind waves. In: The BACC II Author Team, *Second Assessment of Climate Change for the Baltic Sea Basin*, Regional Climate Studies, Springer, Cham, pp. 155–185, doi: 10.1007/978-3-319-16006-1_9.
- Jevrejeva S. 2001. Severity of winter seasons in the northern Baltic Sea between 1529 and 1990: reconstruction and analysis. *Clim. Res.* 17(1): 55–62.
- Jevrejeva S., Drabkin V.V., Kostjukov J., Lebedev A.A., Leppäranta M., Mironov Y.U., Schmelzer N. & Sztobryn M. 2004. Baltic Sea ice seasons in the twentieth century. *Clim. Res.* 25(3): 217–227.
- Kabacoff R. 2011. *R in Action: Data analysis and graphics with R*. Shelter Island, NY, USA: Manning publications.
- Käyhkö J., Apsite E., Bolek A., Filatov N., Kondratyev S., Korhonen J., Kriaučiūnienė J., Lindström G., Nazarova L., Pyrh A. & Sztobryn M. 2015. Recent change–river run-off and ice cover. In: The BACC II Author Team, *Second Assessment of Climate Change for the Baltic Sea Basin*, Regional Climate Studies, Springer, Cham, pp. 99–116, doi: 10.1007/978-3-319-16006-1_5.
- Kelpšaitė-Rimkienė L., Parnell K.E., Žaromskis R. & Kon-

- drat V. 2021. Cross-shore profile evolution after an extreme erosion event—Palanga, Lithuania. *J. Mar. Sci. Eng.* 9(1): 38, doi:10.3390/jmse9010038.
- Komen G.J., Cavaleri L., Donelan M., Hasselmann K., Hasselmann S. & Janssen P.A.E.M. 1996. *Dynamics and Modelling of Ocean Waves*. Cambridge University Press, Cambridge, UK.
- Kudryavtseva N.A. & Soomere T. 2016. Validation of the multi-mission altimeter data for the Baltic Sea region. *Estonian J. Earth Sci.* 65: 161–175, doi: 10.3176/earth.2016.13.
- Kudryavtseva N. & Soomere T. 2017. Satellite altimetry reveals spatial patterns of variations in the Baltic Sea wave climate. *Earth Syst. Dyn.* 8(3): 697–706, doi: 10.5194/esd-8-697-2017.
- Kudryavtseva N., Räämet A. & Soomere T. 2020. Coastal flooding: Joint probability of extreme water levels and waves along the Baltic Sea coast. *J. Coast. Res.* 95(SI): 1146–1151, doi: 10.2112/SI95-222.1.
- Labuz T.A. 2015. Environmental impacts—coastal erosion and coastline changes. In: The BACC II Author Team, *Second Assessment of Climate Change for the Baltic Sea Basin*. Regional Climate Studies, Springer, Cham, pp. 381–396, doi: 10.1007/978-3-319-16006-1_20.
- Lavergne T., Sørensen A. M., Kern S., Tonboe R., Notz D., Aaboe S., Bell L., Dybkjær G., Eastwood S., Gabarro C., Heygster G., Killie A. M., Kreiner B. M., Lavelle J., Saldo R., Sandven S. & Pedersen L.T. 2019. Version 2 of the EUMETSAT OSI SAF and ESA CCI sea-ice concentration climate data records. *Cryosphere* 13(1): 49–78, doi: 10.5194/tc-13-49-2019.
- Lensu M. & Goerlandt F. 2019. Big maritime data for the Baltic Sea with a focus on the winter navigation system. *Mar. Policy* 104: 53–65, doi:10.1016/j.marpol.2019.02.038.
- Leppäranta M. 2012. Ice Season in the Baltic Sea and Its Climatic Variability. In: Haapala I. (ed.), *From the Earth's Core to Outer Space*. Lecture Notes in Earth Sciences, 137. Springer, Berlin, Heidelberg, pp. 139–149, doi:10.1007/978-3-642-25550-2_9.
- Leppäranta M. & Myrberg K. 2009. The ice of the Baltic Sea. In: *Physical Oceanography of the Baltic Sea*. Springer Praxis, Berlin, Heidelberg, pp. 219–260, doi: 10.1007/978-3-540-79703-6_7.
- Liu A.K. & Mollo-Christensen E. 1988. Wave propagation in a solid ice pack. *J. Phys. Oceanogr.* 18(11): 1702–1712, doi: 10.1175/1520-0485(1988)018<1702:WPIASI>2.0.CO;2
- Mäll, M., Nakamura, R., Suursaar, Ü. & Shibayama, T. 2020. Pseudo-climate modelling study on projected changes in extreme extratropical cyclones, storm waves and surges under CMIP5 multi-model ensemble: Baltic Sea perspective. *Nat. Hazards* 102: 67–99, doi: 10.1007/s11069-020-03911-2.
- Männikus R., Soomere T. & Kudryavtseva N. 2019. Identification of mechanisms that drive water level extremes from in situ measurements in the Gulf of Riga during 1961–2017. *Cont. Shelf Res.* 182: 22–36, doi: 10.1016/j.csr.2019.05.014.
- Merkouriadi I. & Leppäranta M. 2014. Long-term analysis of hydrography and sea-ice data in Tvärminne, Gulf of Finland, Baltic Sea. *Clim. Change* 124(4): 849–859, doi:10.1007/s10584-014-1130-3.
- Mostert W. & Deike L. 2020. Inertial energy dissipation in shallow-water breaking waves. *J. Fluid Mech.* 890: A12, doi: 10.1017/jfm.2020.83.
- Najafzadeh F., Kudryavtseva N. & Soomere T. 2021. Effects of large-scale atmospheric circulation on the Baltic Sea wave climate: application of the EOF method on multi-mission satellite altimetry data. *Clim. Dyn.* 57(3–4), doi: 10.1007/s00382-021-05874-x.
- Nikolkina I., Soomere T. & Räämet A. 2014. Multidecadal ensemble hindcast of wave fields in the Baltic Sea. 2014 *IEEE/OES Baltic International Symposium (BALTIC)*, “Measuring and Modeling of Multi-Scale Interactions in the Marine Environment”, May 26–29, Tallinn, Estonia. IEEE Conference Publications, doi: 10.1109/BALTIC.2014.6887854.
- Nilsson E., Rutgersson A., Dingwell A., Björkqvist J.-V., Pettersson H., Axell L., Nyberg J. & Strömstedt E. 2019. Characterization of wave energy potential for the Baltic Sea with focus on the Swedish Exclusive Economic Zone. *Energies* 12(5): 793, doi: 10.3390/en12050793.
- Omstedt A. & Nyberg L. 1996. Response of Baltic Sea ice to seasonal, interannual forcing and climate change. *Tellus A* 48(5): 644–662, doi: 10.3402/tellusa.v48i5.12160.
- Omstedt A., Pettersson C., Rodhe J. & Winsor P. 2004. Baltic Sea climate: 200 yr of data on air temperature, sea level variation, ice cover, and atmospheric circulation. *Clim. Res.* 25(3): 205–216, doi: 10.3354/cr025205.
- Omstedt A., Elken J., Lehmann A., Leppäranta M., Meier H.E.M., Myrberg K. & Rutgersson A. 2014. Progress in physical oceanography of the Baltic Sea during the 2003–2014 period. *Prog. Oceanogr.* 128: 139–171, doi: 10.1016/j.pocean.2014.08.010.
- Orviku K., Jaagus J., Kont A., Ratas U. & Rivis R. 2003. Increasing activity of coastal processes associated with climate change in Estonia. *J. Coast. Res.* 19: 364–375.
- OSI SAF 2017. *Global Sea Ice Concentration Climate Data Record v2.0 — Multimission, EUMETSAT SAF on Ocean and Sea Ice*, doi: 10.15770/EUM_SAF_OSI_0008.
- Overeem I., Anderson R.S., Wobus C.W., Clow G.D., Urban F.E. & Matell N. 2011. Sea ice loss enhances wave action at the Arctic coast. *Geophys. Res. Lett.* 38(17), doi: 10.1029/2011GL048681.
- Pryor S.C. & Barthelmie R.J. 2003. Long-term trends in near-surface flow over the Baltic. *Int. J. Climatol.* 23(3): 271–289, doi: 10.1002/joc.878.
- Räämet A. & Soomere T. 2010. The wave climate and its seasonal variability in the northeastern Baltic Sea. *Estonian J. Earth Sci.* 59(1): 100–113, doi: 10.3176/earth.2010.1.08.
- Räämet A. & Soomere T. 2021. Spatial pattern of quality of historical wave climate reconstructions for the Baltic Sea. *Boreal Environ. Res.* 26: 29–41.
- Ruosteenoja K., Vihma T. & Venäläinen A. 2019. Projected Changes in European and North Atlantic Seasonal Wind Climate Derived from CMIP5 Simulations. *J. Clim.* 32(19): 6467–6490, doi: 10.1175/JCLI-D-19-0023.1.

- Rutgersson A., Kjellström E., Haapala J., Stendel M., Danilovich I., Drews M., Jylhä K., Kujala P., Guo Larsén X., Halsnæs K., Lehtonen I., Luomaranta A., Nilsson E., Olsson T., Särkkä J., Tuomi L. & Wasmund N. 2022. Natural hazards and extreme events in the Baltic Sea region. *Earth Syst. Dynam.* 13(1): 251–301, doi: 10.5194/esd-13-251-2022.
- Ryabchuk D., Kolesov A., Chubarenko B., Spiridonov M., Kurennoy D. & Soomere T. 2011. Coastal erosion processes in the eastern Gulf of Finland and their links with geological and hydrometeorological factors. *Boreal Environ. Res.* 16(Suppl. A): 117–137.
- Seifert T., Tauber F. & Kayser B. 2001. A high resolution spherical grid topography of the Baltic Sea—revised edition. In: *Baltic Sea Science Congress, November 25–29, 2001, Stockholm, Sweden*, Poster 147.
- Sztobryn M. 1994. Long-term changes in ice conditions at the Polish coast of the Baltic Sea. In: *Proc. 12th Int. Symp. on Ice, Norwegian Inst. Techn., Trondheim, Norway, August 23–26, 1994*, 345–354.
- [SMHI and FIMR] 1982. Swedish Meteorological and Hydrological Institute, and Finnish Meteorological Institute. *An Ice Atlas for the Baltic Sea, Kattegat, Skagerrak and Lake Vänern*. Norrköping, Sjöfartsverket.
- Sooäär J. & Jaagus J. 2007. Long-term changes in the sea ice regime in the Baltic Sea near the Estonian coast. *Estonian J. Eng.* 13(3): 189–200.
- Soomere T., Behrens A., Tuomi L. & Nielsen J.W. 2008. Wave conditions in the Baltic Proper and in the Gulf of Finland during windstorm Gudrun. *Nat. Hazards Earth Syst. Sci.* 8(1): 37–46, doi: 10.5194/nhess-8-37-2008.
- Soomere T. & Räämet A. 2011. Long-term spatial variations in the Baltic Sea wave fields. *Ocean Sci.* 7(1): 141–150, doi: 10.5194/os-7-141-2011.
- Soomere T. & Eelsalu M. 2014. On the wave energy potential along the eastern Baltic Sea coast. *Renew. Energy* 71: 221–233, doi: 10.1016/j.renene.2014.05.025.
- Suursaar Ü. & Kullas T. 2009. Decadal variations in wave heights off Cape Kelba, Saaremaa Island, and their relationships with changes in wind climate. *Oceanologia* 51(1): 39–61.
- Suursaar Ü., Kullas T., Otsmann M., Saaremäe I., Kuik J. & Merilain M. 2006. Cyclone Gudrun in January 2005 and modelling its hydrodynamic consequences in the Estonian coastal waters. *Boreal Environ. Res.* 11 (2): 143–159.
- Suursaar Ü., Alari V. & Tõnisson H. 2014. Multi-scale analysis of wave conditions and coastal changes in the north-eastern Baltic Sea. *J. Coast. Res.* 70: 223–228, doi: 10.2112/SI70-038.1.
- Tavakoli S. & Babanin A.V. 2021. Wave energy attenuation by drifting and non-drifting floating rigid plates. *Ocean Eng.* 226: 108717, doi: 10.1016/j.oceaneng.2021.108717.
- Tonboe R.T., Eastwood S., Lavergne T., Sørensen A.M., Rathmann N., Dybkjær G., Pedersen L.T., Høyer J.L. & Kern S. 2016. The EUMETSAT sea ice concentration climate data record. *Cryosphere* 10(5): 2275–2290, doi: 10.5194/tc-10-2275-2016.
- Torralba V., Doblas-Reyes F. J. & Gonzalez-Reviriego N. 2017. Uncertainty in recent near-surface wind speed trends: a global reanalysis intercomparison. *Environ. Res. Lett.* 12(11): 114019, doi: 10.1088/1748-9326/aa8a58.
- Tuomi L., Kahma K. K. & Pettersson H. 2011. Wave hindcast statistics in the seasonally ice-covered Baltic Sea. *Boreal Environ. Res.* 16(6): 451–472.
- Tuomi L., Kanarik H., Björkqvist J.-V., Marjamaa R., Vainio J., Hordoir R., Höglund A. & Kahma K.K. 2019. Impact of ice data quality and treatment on wave hindcast statistics in seasonally ice-covered seas. *Front. Earth Sci.* 7: 166, doi: 10.3389/feart.2019.00166.
- Vihma T. & Haapala J. 2009. Geophysics of sea ice in the Baltic Sea: A review. *Prog. Oceanogr.* 80(3–4): 129–148, doi: 10.1016/j.pocean.2009.02.002.
- Von Storch H., Omstedt A., Pawlak J. & Reckermann M. 2015. Introduction and Summary. In: The BACC II Author Team, *Second Assessment of Climate Change for the Baltic Sea Basin*. Regional Climate Studies, Springer, Cham, pp. 1–22, doi: 10.1007/978-3-319-16006-1_1.
- Zaitseva-Pärnaste I. & Soomere T. 2013. Interannual variations of ice cover and wave energy flux in the north-eastern Baltic Sea. *Ann. Glaciol.* 54(62): 175–182, doi: 10.3189/2013AoG62A228.
- Zhang N., Li S., Wu Y., Wang K.H., Zhang Q., You Z.J. & Wang J. 2020. Effects of sea ice on wave energy flux distribution in the Bohai Sea. *Renew. Energy* 162: 2330–2343, doi: 10.1016/j.renene.2020.10.036.